Frequency Conversion in External Cavity Semiconductor Lasers Exposed to Optical Injection

Elena Cerboneschi, Daniel Hennequin, and Ennio Arimondo

Abstract— **We have investigated experimentally and theoretically the phenomenon of frequency conversion in a semiconductor laser subjected simultaneously to delayed feedback and optical injection. We report observations of frequency conversion in the nearly degenerate detuning range, even with the production of a cascade of higher harmonics, through the process of multiwave mixing. We demonstrate that the external feedback exerts a strong influence on the conversion process, by narrowing the linewidth of the converted signal and, mainly, by affecting the conversion efficiency. Maxima in the efficiency occur whenever the frequency of the injected signal fulfils the phase conditions imposed by the external cavity; moreover, the choice of the feedback parameters controls the detuning range within which frequency conversion is allowed.**

I. Introduction

A SEMICONDUCTOR laser exposed to external perturbations, like delayed feedback and optical injection, is a very interesting system from the point of view of nonlinear dynamics. Although external feedback and optical injection may induce instabilities and chaos [1]–[6], they can be used to improve the spectral properties of semiconductor lasers, i.e., to narrow the linewidth [7] and reduce dynamical chirping. Nonlinear phenomena in optical systems involving semiconductor lasers deserve attention also because of their technological interest, mainly in fiber-optic communications and optical disk applications.

Delayed optical feedback from an external reflector strongly affects dynamical and spectral characteristics of semiconductor lasers. Stable operation with linewidth reduction is achieved at weak feedback levels, when phase matching conditions are fulfilled [7]. The external reflector and the laser facet create an external cavity with its own resonance frequencies. If the feedback level is sufficiently high, several modes of the external cavity, or, more precisely, of the compound system constituted by the semiconductor laser and the external cavity, determine the laser operation [8], leading to either multistability [7], [8] or unstable and chaotic regimes [2]–[4].

Manuscript received March 9, 1995; revised September 27, 1995. This work was supported by the Consiglio Nazionale delle Ricerche with a grant to the Progetto Finalizzato Telecomunicazioni and through the collaboration program with Conseil National Recherche Scientifique of France. The stay of D. Hennequin at the University of Pisa was supported by an EC fellowship.

E. Cerboneschi is with the Dipartimento di Fisica, Università di Pisa, Piazza Torricelli 2, I-56126, Pisa, Italy.

D. Hennequin is with the Laboratoire de Spectroscopie Hertzienne, Unité associée au CNRS, Université des Sciences et Technologies de Lille, 59655 Villeneuve d'Ascq Cedex, France.

E. Arimondo is with the Dipartimento di Fisica, Università di Pisa, Piazza Torricelli 2, I-56126, Pisa, Italy. He is also with JILA, University of Colorado, Boulder, CO 80309-0440 USA.

Publisher Item Identifier S 0018-9197(96)01102-5.

The injection of an external laser field into the cavity of a semiconductor laser can produce injection-locking, i.e., it can force the semiconductor laser to emit a spectrum identical to the injected signal. The stability of the injection-locking regime is strictly limited by the relaxation oscillations, very easily excited. The stable locking range corresponds to a narrow region of injection parameters [9]. Optical injection out of the locking range gives rise to frequency conversion through the process of FWM [10], provided the injected signal is not too intense [6], [11]. Because of the small tranverse dimension of the active layer of semiconductor lasers, FWM occurs in collinear geometry and therefore, it does not modify the transverse spatial distribution of the laser emission and only affects the optical spectrum. The two counterpropagating waves which compose the stationary field inside the cavity of the semiconductor laser act as pump fields and the injected external field as a probe field. The interference of the probe field with one of the two pump waves induces a modulation, i.e., a grating, in the refractive index of the semiconductor medium. The scattering of the second pump wave on such a grating produces a conjugate wave. The energy and momentum conservation rule requires that, if ω_0 and ω_i are the oscillation frequencies of pump and probe fields respectively, the frequency ω_f of the FWM generated wave satisfies the relation $\omega_0 - \omega_i = \omega_f - \omega_0$. Therefore, the FWM spectrum consists in a strong central component at the ω_0 oscillation frequency of the free-running laser, the pump field, and two weaker components at the ω_i injection frequency of the probe field and at the ω_f frequency of the conjugate wave, symmetric with respect to the main component.

Frequency conversion through FWM has been extensively studied in recent years both in semiconductor lasers [10]–[18] and travelling wave semiconductor optical amplifiers [19]–[22]. Two types of FWM have been classified. When the detuning between pump and injected fields is smaller than the frequency separation of the resonance modes of the laser cavity, i.e., in the case of intramodal injection [17], FWM is defined as nearly degenerate. For intermodal injection, with detuning values larger than the mode separation, FWM is currently indicated as highly nondegenerate. For nearly degenerate FWM the detuning values range up to ten GHz [13]; for highly nondegenerate FWM, they can exceed the THz [15], [16]. In the two FWM processes different nonlinear interactions between electromagnetic field and semiconductor medium are involved. In nearly degenerate FWM the refractive index modulation, responsible for the production of the conjugate field component, is due to the

pulsations of the carrier number at the beat frequency between pump and injected field [14]. In semiconductor lasers the efficiency in the nearly degenerate FWM process resonantly increases when the detuning approaches the frequency of the coupled field-carrier number relaxation oscillations [18]. In connection with the dynamics of the carrier number, resonant enhancement of FWM frequency conversion has been demonstrated also in semiconductor optical amplifiers [20]: the conversion efficiency increases considerably if the bias current is modulated at a frequency equal to the detuning between pump and probe fields. In the highly nondegenerate detuning range the FWM frequency conversion is due to the gain saturation produced by ultrafast processes in the field-medium interaction. Among such processes, whose characteristic times are in the 0.1 to 1 ps range, carrier heating and spectral hole burning have been identified [22]. It has been shown that highly nondegenerate FWM occurs only for detuning values close to multiples of the frequency separation between resonance modes of the laser cavity, in other words if the frequency of the injected field matches a resonance mode of the semiconductor laser.

We have examined experimentally for the first time the combined effect of optical feedback from an external cavity and optical injection on a semiconductor laser. Our experimental configuration, with simultaneous feedback and injection, corresponds to realistic operating conditions in most of the applications where optical injection is employed; in fact, external feedback is present in several applications of semiconductor lasers, for instance when they are coupled to optical fibers. In our operating conditions, the feedback parameters are chosen such that stable emission of the semiconductor laser, with linewidth reduction, is obtained. At the same time, optical injection of an external laser field is applied. We have performed experimental observations of nearly degenerate FWM and multiwave mixing on our apparatus. We have pointed out the twofold effect of the optical feedback in the frequency conversion process. On one hand, a reduction of the linewidth of the converted signal is produced. On the other, a modulation of both efficiencies of transmission of the signal at the injection frequency and conversion at the conjugate frequency, as functions of the detuning, is originated. This modulation occurs with a frequency equal to the free spectral range of the external cavity which supplies the feedback.

We have also extended the well known Lang–Kobayashi model to analyze the frequency conversion process in our experimental conditions. Within the delay rate equations for a semiconductor laser with external feedback [23], we have added a term which describes the external light injection.[1] Our extended model well reproduces the observed modulation of the transmission and conversion efficiencies. Moreover, on the basis of the calculated efficiencies, we show that the feedback parameters allow us to control, to a certain extent, the detuning range where frequency conversion takes place. Our theoretical analysis is concentrated on the observed features of the FWM process, even if multiwave mixing has been also observed experimentally.

[1] In a paper published after the present one was submitted [24], similar equations have been considered to analyze the transient dynamics of diode lasers operating in presence of both optical feedback and external light injection.

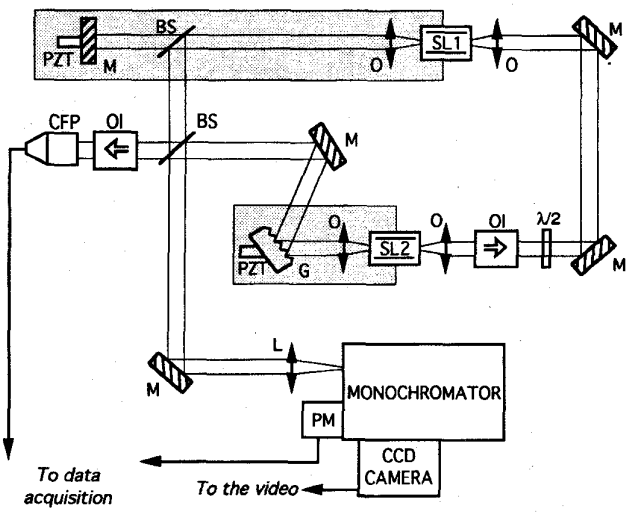

Fig. 1. Experimental setup. SL1 and SL2: semicondutor lasers; O: objectives; BS: beam splitters; M: mirrors; G: grating; L lens; CFP: confocal Fabry-Perot spectrum analyzer; OI: optical isolator; $\lambda/2$: half-wave retard plate; PM photomultiplier: PZT: piezoelectric transducers.

Our analysis is similar to the recently published theoretical description of the FWM process in an injection-locked semiconductor laser [25]. In the configuration examined in this reference, the FWM pump field is provided by a semiconductor laser frequency-locked through optical injection of an external field. Another external field, injected outside the locking range, acts as probe signal for the FWM process. Such a system is similar to our FWM configuration, where the FWM pump field is provided by the semiconductor laser field frequency-locked by the external cavity. In fact, under proper conditions for stable emission [26], an external optical feedback leads to self-locking of the semiconductor laser field.

The present paper is organized as follows. Section II describes the experimental configuration and reports the experimental observations of frequency conversion in the presence of simultaneous optical feedback. The observed effect of the optical feedback on the FWM efficiency is also described in Section II. In Section III we introduce our model of FWM in the presence of optical feedback and discuss the theoretical results. The conclusions and future perspectives are presented in Section IV.

II. Experiment

A. Apparatus

The experimental setup is sketched in Fig. 1. Two lasers Hitachi HLP1400, oscillating at wavelengths around 830 nm, have been used. Such lasers emit from both front and rear facets, with a maximum power of some tens of mW. The laser indicated as SL1 in the figure is subjected to optical injection and external feedback on its rear and front facets, respectively. SL1 laser will be denoted in the following also as pump laser. The beam emitted from the front facet (on the left hand, in the figure) is collimated with an antireflection coated objective

and successively reinjected into the internal cavity of the laser by means of a flat high reflectivity mirror, placed 68 cm apart and mounted on a piezoelectric transducer. We indicate as external cavity the cavity composed by the front facet of the semiconductor laser and the mirror which faces it. The FSR of the external cavity is 220 MHz. A calibrated attenuator is inserted into the cavity when required. A fraction of the laser intensity is extracted from the external cavity by means of a beam splitter and used for the detection. The radiation emitted by another laser, denoted as SL2, is injected through the rear facet (on the right in the figure). The beam coming from the rear facet of SL2 is first collimated, then sent through a half-wave retardation plate, to achieve polarization matching with the field of the laser SL1, and finally focused onto SL1. An optical isolator prevents the radiation emitted by SL1 being injected into SL2 in turn. The laser SL2 is spectrally stabilized by means of an external grating cavity. Rotation of the grating allows us to obtain discrete variations of the SL2 frequency, while translation of the grating through a piezoelectric allows a continuous frequency shift. The tuning of the SL2 bias current realizes the final continuous control of the frequency for the injected signal.

The SL1 laser diode has a free-running laser threshold of 56.7 mA. The experimental results here reported have been obtained with laser current at 81.7 mA, corresponding to a laser output power of 17 mW. The FWM observations have been performed in conditions of very weak feedback from the external cavity, with effective reflectivity of the external cavity, including coupling losses and attenuation, of -43 dB. This value locates the laser diode operation in the feedback-phase sensitive monomode regime described in ref. [7] and between the regimes II and III of the phase-diagram introduced by Tkach-Chraplyvy [8]. The output power of the SL2 laser is 1 mW and only four percent of it is extimated to be coupled into the SL1 cavity.

Spectral analysis of the radiation emitted by the two lasers is performed by means of a confocal scanning Fabry–Perot spectrum analyzer, having 1.5 GHz FSR, and of a monochromator with 0.01 nm maximum resolution. The monochromator has been used to monitor the optical spectra of both lasers and tune their wavelengths, while the FWM spectra have been observed, with relatively high resolution, by means of the spectrum analyzer.

B. FWM Experimental Observation

In the Fabry-Perot spectra of the emission of the laser SL1, we could appreciate directly the effects of the external feedback by simply switching the feedback on and off. Fig. 2 shows FWM spectra corresponding to the same operating conditions except for the feedback, which is off in Fig. 2(a) and on in Fig. 2(b). The total frequency scan in these figures is slightly larger than the Fabry–Perot FSR and the peaks at the left and right edges of the horizontal axes correspond to the same laser frequency matching two successive modes of the scanning Fabry–Perot spectrum analyzer. The zero detuning has been arbitrarily fixed at the frequency of the SL2 injection laser. The corresponding peak in the SL1 FWM

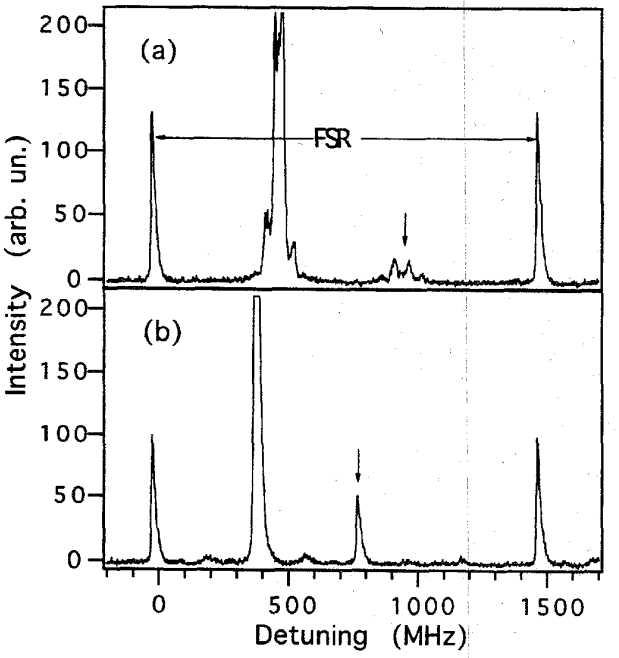

Fig. 2. Output from the 1.5 GHz FSR Fabry–Perot spectrum analyzer, showing FWM frequency conversion in the semiconductor laser subjected to optical injection (a) without and (b) with simultaneous external feedback. The feedback-induced reduction of the linewidth of the pump laser directly affects the central component of the spectrum and is transmitted to the converted signal. The zero frequency on the horizontal axis corresponds to the frequency of the injected signal. The arrow marks the field component at the conjugate frequency.

spectra represents the transmission of the injected probe field. The largest peak in Fig. 2(a) corresponds to the FWM pump signal provided by the laser SL1 in the absence of optical feedback. This peak reproduces the spectrum of the free-running laser, apart from a frequency shift induced by the injection of the external signal. We have observed a frequency shift of the central component of the FWM spectrum with respect to the free-running laser by comparing the Fabry–Perot spectra of SL1 laser recorded either with or without optical injection. The observed shift is not produced, as suggested in [12], by the variation in the carrier number induced by the injected field on the pump laser: that frequency shift would change its sign depending on the relative detuning of SL2 with respect to SL1. On the contrary, in our case the frequency shift is always negative; thus, a larger shift, masking the one described in [12], is induced by an additional process, which could be the heating of the pump laser produced by the injection beam. The spectrum of Fig. 2(a) evidences that the pump field emitted by the laser in the absence of optical feedback is affected by a frequency jitter. This frequency jitter is transmitted to the FWM generated output signal, represented in the figure by the weak multipeaked structure marked by the arrow. In Fig. 2(b), the largest peak represents the pump field emitted by the SL1 laser in the presence of optical feedback from the external cavity. Because of the external feedback, the laser linewidth is narrowed and the frequency jitter suppressed. As stated above, in order to achieve a stable emission we have operated SL1 laser in weak feedback

conditions; moreover, the feedback phase has been chosen, by means of a fine adjustment of the length of the external cavity with the piezoelectric transducer, to achieve the largest linewidth reduction [7]. In the spectrum shown in Fig. 2(b) the pump field frequency is slightly shifted with respect to the spectrum in Fig. 2(a), due to the external optical feedback. This feedback-induced change in the oscillation frequency is explained by the fact that the coupling of the semiconductor laser to the external cavity changes both the phase condition imposed on the laser field and the gain. We must also specify that the two different frequency shifts mentioned above add up as independent effects of optical injection and feedback to give the actual position of the pump field in the simultaneous presence of injection and feedback. We have verified that both shifts are not related to drifts of the SL1 laser frequency. The spectrum of Fig. 2(b) contains weak sidebands separated in frequency from the pump field component by the 220 MHz FSR of the external cavity. These sidebands, observed also in [7], are induced by the external feedback and correspond to the resonance modes of the external cavity closest to the excited mode. The lineshape of the FWM conjugate output is the convolution of the pump and the injected signals. Therefore, the linewidth narrowing and the frequency jitter suppression of the pump signal are transmitted to the field component at the conjugate frequency, as clearly seen in Fig. 2(b), where the conjugate field is indicated by the arrow.

Because of the 1.5 GHZ FSR of our spectrum analyzer, the detuning between pump and injected fields was not precisely determined. The detuning was always smaller than the 0.01 nm (i.e., 5 GHz) resolution of the monochromator, employed to monitor the optical spectra simultaneously with the Fabry–Perot spectrum analyzer. In fact, the wavelengths of the two lasers SL1 and SL2, monitored at the same time, could not be resolved by the monochromator. Thus, the frequency difference between the pump and injected signals, as monitored through the spectrum analyzer, was determined with an uncertainty up to three Fabry–Perot FSR. Our detuning values correspond to the nearly degenerate range.

In Fig. 3, we show some typical frequency conversion spectra observed with the pump laser exposed to optical feedback, for increasing detuning of the injected laser. These spectra are composed of the main peak corresponding to the pump signal, a peak at the frequency of the injected signal, always used as the zero of the detuning scale, and several converted signals on both sides of the central component. Spectra were obtained from the Fabry–Perot output, so that its 1.5 GHz FSR defines the horizontal scale. The secondary converted signals, which are separated from the main peak by multiples of the detuning between pump and probe, are produced as a cascade of higher harmonics through a multiwave mixing process [14]. We have observed up to the third harmonic, as shown in Fig. 3(b) (on both sides of the pump peak) and in Fig. 3(c) (only on the left side). As we will discuss in the following, the intensities of the field components, at the injection frequency, at the conjugate frequency and higher harmonics, display an oscillatory behavior as functions of the detuning. In the specific case depicted in the figure, the oscillation is particularly evident for the first hamonic converted signal (the first peak

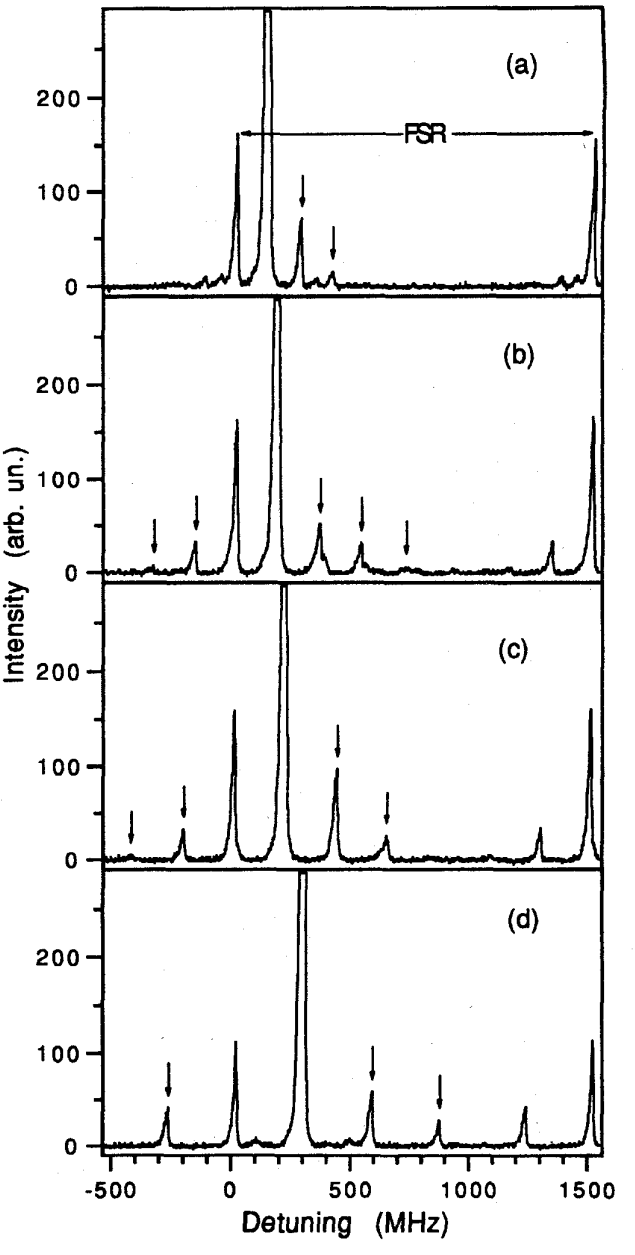

Fig. 3. Output from the Fabry–Perot spectrum analyzer showing nearly degenerate multiwave mixing with cascade production of converted signals in the external cavity semiconductor laser. Spectra (a) to (d) correspond to increasing values of the SL2-SL1 relative detuning. The absolute detuning is know apart from a multiple (at maximum three) of the 1.5 GHz spectrum analyzer FSR; the zero on the horizontal axis corresponds to the frequency of the injected signal. The converted signals are marked by arrows.

on the right side of the pump field, in the figure). We see that, passing from Fig. 3(a) to (d), its intensity first decreases, then grows and finally decreases again. From Fig. 3(a) to (d), the variation of the detuning between injected and pump field is within one FSR of the external cavity. We notice that, in the series of graphs reported in the figure, the relative intensities of the different frequency components are not the same at different detuning values. For example, in Fig. 3(b) and (d) the intensities of the second-harmonic converted signals are

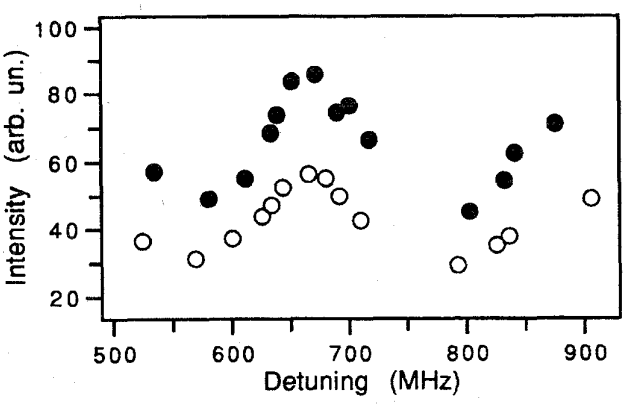

Fig. 4. Intensities of the transmitted probe signal (filled circles) and of the FWM converted signal (open circles) as functions of the detuning between the pump and the injected fields. The detuning is derived from the FWM spectra, and includes the shift induced on the pump frequency by optical injection and external feedback; for its absolute value, see Fig. 3.

comparable to those of the first harmonic, while in Fig. 3(a) and (c), they are sensibly lower. Similarly, the appearance of the third harmonic is not necessarily accompanied by higher efficiency in the production of the first-harmonic converted signal. In fact, we can see third harmonics both in Fig. 3(b) and (c), with first harmonics having low and high intensity, respectively.

C. Feedback Effects on the Frequency Conversion Efficiency

Among the different features of the frequency generation process, pointed out from the experimental spectra shown in Fig. 3, we concentrate on the intensity oscillations of the different components of the multiwave mixing spectra versus the detuning between injected and pump fields. From the multiwave mixing spectra, recorded with the pump laser exposed to optical feedback and for different detuning between the pump and injected fields, in Fig. 4 the intensities of the field components at the injected frequency and at the FWM conjugate frequency are reported as functions of the SL2–SL1 relative detuning. The curves display maxima and minima, separated in frequency by the FSR of the external cavity. The intensities of the higher harmonic converted signals, which appear in the spectra shown in Fig. 3, follow the same oscillating behavior as functions of the detuning. These oscillations are induced by the external optical feedback and disappear when the feedback is switched off.

The feedback modifies the spectral characteristics of a semiconductor laser by producing resonances on a fine structure of modes determined by the FSR of the external cavity. An intense optical feedback may induce the simultaneous excitation of the laser on many of such modes, as observed for instance in [27]. In our feedback conditions, only one laser mode oscillates, while all the other ones remain below the laser threshold. Nevertheless, any external perturbation, like the optical injection, causes the system, composed by the laser and the external cavity, to respond resonantly on these modes. As a consequence, in the frequency conversion process maxima in efficiency occur when the injected signal matches the phase conditions imposed on the electromagnetic field by the external cavity. This simple picture explains the oscillating response in the multiwave mixing generation. Furthermore, it is confirmed by the theoretical model presented in the next section. Thus, our results on frequency conversion in semiconductor lasers exposed to optical feedback demonstrate that the FWM and multiwave mixing conjugate outputs are enhanced by the resonances introduced by the external cavity in the laser system. Resonant enhancement of the frequency conversion efficiency has been demonstrated in other semiconductor laser configurations, as well. We remind, for instance, that in [10], [12], [18], and [25] the maximum efficiency in the FWM frequency conversion was obtained with detuning equal to the relaxation oscillation frequency. In [16] and [15], for the highly nondegenerate FWM, only when the injection frequency was adjusted to one of the resonance modes of the laser cavity, a converted signal was found at the corresponding mode on the other side of the spectrum. Finally in [20], FWM resonant enhancement was demonstrated in semiconductor amplifiers through the modulation of the bias current.

III. Theory

The rate equations of Lang-Kobayashi [23] properly describe the behavior of a semiconductor laser exposed to delayed optical feedback. In that model the equation for the complex electric field $\mathcal{E}(t)$ is written as:

$$\dot{\mathcal{E}}(t) = \frac{1}{2}[\Gamma G(N) - \Gamma_0]\mathcal{E}(t) + i\Omega(N)\mathcal{E}(t) + \kappa_f \mathcal{E}(t-\tau) + \kappa_i \mathcal{E}_i(t). \quad (1)$$

In this equation a term describing the injection of the external field $\mathcal{E}_i(t)$ is included. N represents the number of charge carriers in the laser active layer; the optical gain per time unit is represented by $\Gamma G(N)$, where Γ is the confinement factor and $G(N)$ the gain of the carrier number; the optical losses per time unit are indicated as Γ_0; $\Omega(N)$ is the carrier number dependent oscillation angular frequency; κ_f and κ_i are the feedback coefficient and the injection coupling coefficient, respectively; τ is the roun-dtrip time of the external cavity. The feedback term in (1), delayed by the round-trip time τ of the external cavity, only allows for a single reflection from the external mirror and properly represents weak feedback intensities. High feedback levels are described by taking into account multiple reflections [28], [29].

The coupling coefficients κ_f [30] and κ_i [31] read

$$\kappa_f = \frac{1-R}{\tau_{in}}\sqrt{\frac{R_{\text{ext}}}{R}} \quad (2)$$

$$\kappa_i = \frac{1-R'}{\tau_{in}\sqrt{R'}}, \quad (3)$$

where τ_{in} is the round-trip time of the internal cavity of the semiconductor laser, R_{ext} and R are the reflectivities of the external mirror and of the laser facet facing it respectively, R' is the reflectivity of the laser facet through which the external signal is injected. We perform a series expansion of the optical gain and the angular frequency around the threshold carrier number of the free-running laser N_{th}:

$$\Gamma G(N) = \Gamma_0 + \Gamma G_N(N - N_{th}) \quad (4)$$

$$\Omega(N) = \omega_0 + \frac{1}{2}\alpha\Gamma G_N(N - N_{th}), \tag{5}$$

where $G_N = \partial G/\partial N$ is the differential gain, ω_0 is the oscillation angular frequency of the free-running laser and α is the linewidth enhancement factor. By writing the electric fields of the pump laser $\mathcal{E}(t)$ and of the injected signal $\mathcal{E}_i(t)$ as:

$$\mathcal{E}(t) = E(t)\exp(i\omega_0 t) \tag{6}$$

$$\mathcal{E}_i(t) = E_i(t)\exp(i\omega_i t) \tag{7}$$

and using (4) and (5), the rate equation for the electric field amplitude becomes

$$\dot{E}(t) = \frac{1}{2}(1 + i\alpha)\Gamma G_N[N(t) - N_{th}]E(t) + \kappa_f e^{-i\omega_0\tau}E(t-\tau) + \kappa_i E_i(t)e^{i(\omega_i-\omega_0)t}. \tag{8}$$

Equation (8) must be coupled to the following rate equation for the carrier number [30]:

$$\dot{N}(t) = J - \frac{N(t)}{\tau_e} - \left\{\frac{\Gamma_0}{\Gamma} + G_N[N(t) - N_{th}]\right\}|E(t)|^2, \tag{9}$$

where J is the carrier bias rate and τ_e the carrier lifetime.

In order to study the frequency conversion process, we use the following ansatz for the electric field and the carrier number:

$$E(t) = E_0 + \epsilon_1 e^{i(\omega_i-\omega_0)t} + \epsilon_2 e^{-i(\omega_i-\omega_0)t} \tag{10}$$

$$N(t) = N_{th} + n_0 + ne^{i(\omega_i-\omega_0)t} + n^* e^{-i(\omega_i-\omega_0)t}, \tag{11}$$

where the higher harmonics $\pm m(\omega_i - \omega_0)$, with $m = 2, 3, \cdots$, are neglected. We disregard also, for simplicity, the frequency shift of the central component of the FWM spectrum, mentioned in the experimental observations, since it does not produce essential changes in the present analysis. Main aim of the present analysis is to determine, as functions of the detuning $\omega_i - \omega_0$, the amplitudes of the field components at the injected and conjugate frequencies, described by the amplitudes ϵ_1 and ϵ_2 respectively, and to study their dependence on the external optical feedback parameters. By substituting (10) and (11) into (8) and (9), and equating terms with the same time dependence, we obtain the following equations for the field and carrier number components:

$$\dot{E}_0(t) = \frac{1}{2}(1 + i\alpha)\Gamma G_N n_0(t)E_0(t) + \kappa_f E_0(t-\tau)e^{-i\omega_0\tau} \tag{12}$$

$$\dot{\epsilon_1}(t) = -i(\omega_i - \omega_0)\epsilon_1(t) + \frac{1}{2}(1 + i\alpha)\Gamma G_N[n_0(t)\epsilon_1(t) + n(t)E_0(t)] + \kappa_f\epsilon_1(t-\tau)e^{-i\omega_i\tau} + \kappa_i E_i(t) \tag{13}$$

$$\dot{\epsilon_2}(t) = i(\omega_i - \omega_0)\epsilon_2(t) + \frac{1}{2}(1 + i\alpha)\Gamma G_N[n_0(t)\epsilon_2(t) + n^*(t)E_0(t)] + \kappa_f\epsilon_2(t-\tau)e^{-i(2\omega_0-\omega_i)\tau} \tag{14}$$

$$\dot{n_0}(t) = J - \frac{N_{th} + n_0(t)}{\tau_e} - \left[\frac{\Gamma_0}{\Gamma} + G_N n_0(t)\right]|E_0(t)|^2 \tag{15}$$

$$\dot{n}(t) = -i(\omega_i - \omega_0)n(t) - \frac{n(t)}{\tau_e} - G_N n(t)|E_0(t)|^2 + \left[\frac{\Gamma_0}{\Gamma} + G_N n_0(t)\right][E_0(t)\epsilon_2^*(t) + E_0^*(t)\epsilon_1(t)], \tag{16}$$

where the condition $|\epsilon_1|^2, |\epsilon_2|^2 \ll |E_0|^2$ is assumed, which is consistent with neglecting the higher harmonics.

A. Steady-State Solutions

From (12) and (15), by putting the time derivatives equal to zero and, in (12), $E_0(t-\tau) = E_0(t)$, we obtain the steady state solutions for n_0 and E_0:

$$n_0 = -\frac{\kappa_f\cos(\omega_0\tau)}{\frac{1}{2}\Gamma G_N} \tag{17}$$

$$|E_0|^2 = \frac{J - \frac{N_{th}+n_0}{\tau_e}}{\frac{\Gamma_0}{\Gamma} + G_N n_0}. \tag{18}$$

The dc component n_0 of the carrier number represents the modification in the lasing threshold induced by the feedback and, for $-\pi/2(mod2\pi) \leq \omega_0\tau \leq \pi/2(mod2\pi)$, leads to a reduction in the laser threshold. The length of the external cavity may be tuned so that the feedback phase $\omega_0\tau$ leads to the maximum threshold reduction.

The steady-state solution of (16) for the carrier number component oscillating at $\omega_i - \omega_0$ reads:

$$n = -\frac{\frac{\Gamma_0}{\Gamma} + G_N n_0}{i(\omega_i - \omega_0) + 2\lambda_R}(E_0\epsilon_2^* + E_0^*\epsilon_1), \tag{19}$$

where we have introduced the decay rate of the relaxation oscillation λ_R, given by [30]

$$\lambda_R = \frac{1}{2}\left(\frac{1}{\tau_e} + G_N|E_0|^2\right). \tag{20}$$

Actually, (20) gives the feedback modified relaxation oscillation damping rate, since the modified laser intensity of (18) is used in the definition. We define also the modified squared relaxation oscillation frequency as

$$\omega_R^2 = \Gamma_0 G_N|E_0|^2. \tag{21}$$

By using (19), the steady-state equations for the ac components of the electric field become

$$c_1\epsilon_1 + c_2\epsilon_2^* = -\kappa_i E_i \tag{22}$$

$$c_3\epsilon_2 + c_4\epsilon_1^* = 0, \tag{23}$$

where

$$c_1 = -i(\omega_i - \omega_0) - \frac{(1 + i\alpha)\omega_R^2}{2[2\lambda_R + i(\omega_i - \omega_0)]} + \frac{1}{2}(1 + i\alpha)\Gamma G_N(1 - x)n_0 + \kappa_f e^{-i\omega_i\tau} \tag{24}$$

$$c_2 = -\frac{(1 + i\alpha)\omega_R^2}{2[2\lambda_R + i(\omega_i - \omega_0)]} - \frac{1}{2}(1 + i\alpha)\Gamma G_N x n_0 \tag{25}$$

$$c_3 = i(\omega_i - \omega_0) - \frac{(1 + i\alpha)\omega_R^2}{2[2\lambda_R - i(\omega_i - \omega_0)]} + \frac{1}{2}(1 + i\alpha)\Gamma G_N(1 - x^*)n_0 + \kappa_f e^{i(\omega_i-2\omega_0)\tau} \tag{26}$$

TABLE I
PARAMETERS USED IN THE CALCULATIONS

Parameter	Symbol	Value
Oscillation angular frequency	ω_0	2.3 10^{15} s^{-1}
Differential gain	G_N	2.0 10^4 s^{-1}
Threshold carrier number	N_{th}	1.4 10^8
Confinement factor	Γ	0.2
Photon decay rate	Γ_0	3.6 10^{11} s^{-1}
Linewidth enhancement factor	α	5.0
Carrier lifetime	τ_e	1.1 10^{-9} s
Internal cavity roundtrip time	τ_{in}	8.0 10^{-12} s
Facet reflectivity	R, R'	0.32
External cavity roundtrip time	τ	4.5 10^{-9} s

$$c_4 = -\frac{(1+i\alpha)\omega_R^2}{2[2\lambda_R - i(\omega_i - \omega_0)]} - \frac{1}{2}(1+i\alpha)\Gamma G_N x^* n_0. \tag{27}$$

We have indicated as x the complex adimensional quantity

$$x = \frac{G_N |E_0|^2}{2\lambda_R + i(\omega_i - \omega_0)}. \tag{28}$$

The last two terms in (24) and (26) and the last ones in (25) and (37) are related to the external feedback, since they are proportional either to the feedback-induced threshold reduction n_0 or to the feedback coupling parameter κ_f. It is interesting to point out that algebraic equations of the same kind as (22) and (23) are obtained in the theoretical analysis presented in [25].

From (22) and (23), we find the following expressions for the ac components of the electric field:

$$\epsilon_1 = -\frac{c_3^* \kappa_i E_i}{c_1 c_3^* - c_2 c_4^*} \tag{29}$$

$$\epsilon_2 = \frac{c_4 \kappa_i E_i}{c_1^* c_3 - c_2^* c_4}, \tag{30}$$

from which we obtain the efficiencies T of transmission of the signal at the injection frequency ω_i and C of conversion at the conjugate frequency $2\omega_0 - \omega_i$, as

$$T = \left| \frac{\epsilon_1}{E_i} \right|^2 \tag{31}$$

$$C = \left| \frac{\epsilon_2}{E_i} \right|^2. \tag{32}$$

In absence of external feedback, in the limit $n_0, \kappa_f \to 0$, (29) and (30) lead to the same expressions as those reported in [12], if we put equal to zero the injection induced shift of the central frequency component, which was taken into account there.

B. Results and Discussion

We have evaluated the transmission efficiency T and the FWM conversion efficiency C by using the parameters listed in Table I, which are typical for a GaAs–AlGaAs Fabry–Perot laser and apply to our experimental conditions, assuming for ω_0 a value corresponding to the maximum threshold reduction. The resulting curves for the conversion efficiency as a function of the detuning $(\omega_i - \omega_0)/2\pi$ are shown in Fig. (5), for two different values of the optical feedback coupling parameter κ_f and for fixed conditions of bias current and injection intensity. For the carrier number bias rate J we used the value $J = 1.4\ J_{th}$, with $J_{th} = N_{th}/\tau_e$ the threshold bias rate of the free-running laser, and for the injection coefficient the value $\kappa_i = 1.5 \times 10^{11}\ s^{-1}$, derived from (3) with the parameter values listed in Table I. The curves of conversion efficiency, which are reported in the figure only for positive detuning, are symmetrical with respect to zero. The FWM description does not make sense in the locking range, i.e., in a certain interval, determined by the injection parameters, around the zero detuning [9]. Thus the conversion efficiency near the zero detuning should not be considered.

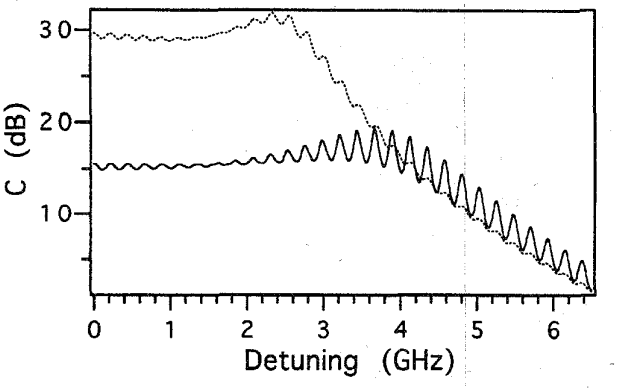

Fig. 5. Theoretical FWM conversion efficiency C, in dB, as a function of the detuning, in GHz, for different values of the feedback coupling parameter: the solid line corresponds to $\kappa_f = 1.3 \times 10^9\ s^{-1}$, equivalent to a feedback effective reflectivity of −41 dB, and the dashed line to $\kappa_f = 5.0 \times 10^8\ s^{-1}$, equivalent to −50 dB reffective reflectivity. The carrier number bias rate has been assumed as $J = 1.4\ J_{th}$ and the injection parameter as $\kappa_i = 1.5 \times 10^{11}\ s^{-1}$. The curves are symmetrical with respect to zero and are reported versus positive detuning only.

As experimentally observed, the conversion efficiency shows an oscillating dependence on the detuning, with frequency equal to the FSR of the external cavity. The depth of this modulation increases with the optical feedback coupling parameter. The oscillations are superimposed to a broad detuning dependence, which displays a resonance when the detuning is equal to the feedback modified relaxation oscillation frequency $\nu_R = \omega_R/2\pi$, with ω_R defined by (21). In nearly degenerate FWM, the same broad dependence of the conversion efficiency, for detuning close to the relaxation oscillation frequency, has been reported in [12], [18] for a semiconductor laser in a standard configuration of optical injection and in [25] for an injection-locked semiconductor laser.

As can be seen from Fig. 5, for detuning values larger than the relaxation oscillation frequency, the conversion efficiency rapidly decreases. Therefore, as pointed out also in [25], we can state that the FWM bandwidth, i.e., the detuning range within which the FWM occurs, is determined by the relaxation oscillation frequency. As a consequence, any parameter which affects this frequency can be used to modify the FWM detuning range. Fig. 5 shows that, with increasing feedback level, the resonance maximum shifts toward higher frequency

detunings. At the same time, a considerable decrease of the absolute efficiency occurs. The shift of the resonance is accompanied by an extension of the FWM bandwidth on the side of the high detunings. In the figure the curves corresponding to the feedback parameters $\kappa_f = 1.3 \times 10^9$ s^{-1} (solid line) and $\kappa_f = 5.0 \times 10^8$ s^{-1} (dashed line) are compared. The curve at higher feedback level, although below the other one at small detunings, is above it at detunings larger than the relaxation frequency. Actually, at high feedback levels, the gain in efficiency at large detuning occurs when the detuning matches the resonances of the external cavity, i.e., at the maxima of the feedback-induced modulation.

We have calculated also the transmission efficiency T, which displays the same oscillations with the detuning at the frequency of the FSR of the external cavity, superimposed to the resonance structure around the relaxation oscillation frequency. Unlike the conversion efficiency, the transmission curve is not symmetrical with respect to zero: it is lower than the corresponding conversion curve for positive detuning and higher for negative detuning. Nevertheless, transmission and conversion efficiencies remain comparable to each other in all the detuning range. The asymmetry becomes more pronounced with increasing feedback level. The same asymmetry in the resonance structure of the transmission efficiency curve has been also pointed out for semiconductor lasers in the absence of optical feedback [12] and is due to the phase-amplitude coupling parameter α. Such an asymmetry concerns, in general, the resonant response of the semiconductor laser system to perturbations and noise. In fact, it also appears in the optical spectrum, where the relaxation oscillations excited by the noise of spontaneous emission produce asymmetrical weak bands at each side of the emission line [32].

Theoretical predictions about the relative efficiency of transmission and conversion in the FWM process have not been definitly confirmed experimentally. In fact, experimental observations of higher efficiency in the transmission than in the conversion for positive detuning, contrary to what expected from the theory, have been published, for instance in [14]. On this subject, our experimental data cannot be compared to the theoretical results because of the experimental uncertainty which, as explained before, affects the determination of the detuning and prevents us from establishing its sign.

IV. Conclusion

We have presented an experimental and theoretical investigation of frequency conversion in the nearly degenerate detuning range, in a semiconductor laser subjected simultaneously to weak feedback from an external cavity and optical injection. Frequency conversion through FWM, and also through multiwave mixing with the production of a cascade of higher harmonic generated signals, has been experimentally observed. As effects of the external feedback on the frequency conversion process, we have shown i) the linewidth reduction of the converted signals, ii) the sinusoidal modulation of the transmission and conversion efficiencies, as functions of the detuning between pump and injected fields, with frequency equal to the FSR of the external cavity. The phase condition imposed by the external cavity on the laser field is responsible for the modulation of the efficiency in transmission and conversion: a maximum occurs whenever the frequency of the injected signal matches the external cavity condition.

A theoretical model of the FWM process in a semiconductor laser under external feedback conditions has been developed, by extending the delay rate equations of Lang–Kobayashi for a semiconductor laser with external feedback. Our analysis confirms the experimental observation that the plot of the FWM efficiency versus detuning presents a feedback-induced oscillation. Our FWM scheme with the pump field supplied by a semiconductor laser subjected to optical feedback resembles to the FWM scheme examined in [25], for an injection-locked semiconductor laser. The similarity of the two systems leads to quite similar model equations and similar mathematical treatment of the FWM problem. Our results confirm those obtained in [25] about the feasibility of a control of the FWM bandwidth by means of a proper choice of the external parameters which affect the relaxation oscillation frequency. New features of our FWM configuration, compared to those of the system examined in [25], are the resonances introduced by the external cavity in the laser system, which modify the efficiency of the FWM process.

In our theoretical treatment, we assume weak injection intensity such that FWM gives a sufficiently accurate description of the laser-medium interaction. This approximation allows an analytical derivation of the efficiencies of FWM transmission and conversion. Some experimental features, such as the multiwave mixing phenomenon, are not allowed for by our model. The observation of multiwave mixing indicates that the approximation of low injection level does not apply to our experimental conditions. For a more comprehensive description of the observed phenomena, a theoretical model that retains the full nonlinearity of the field-medium interaction is required. The gain saturation should be included and the approximation of weak injection level abandoned. Moreover, instead of considering monochromatic laser fields, the sidebands in the optical spectrum of the pump laser and the spontaneous emission noise, which have been shown to add new features in the optical injection, expecially in conditions of high injection power [6], should be considered.

References

[1] J. Sacher, D. Baums, P. Panknin, W. Elsässer, and E. O. Göbel, "Intensity instabilities of semiconductor lasers under current modulation, external light injection, and delayed feedback," *Phys. Rev. A*, vol. 45, pp. 1893–1905, 1992.

[2] D. Lenstra, B. H. Verbeek, and A. J. den Boef, "Coherence-collapse in single-mode semiconductor lasers due to optical feedback," *IEEE J. Quantum Electron.*, vol. QE-21, pp. 674–679, 1985.

[3] J. Mørk, B. Tromborg, and J. Mark, "Chaos in semiconductor lasers with optical feedback: theory and experiment," *IEEE J. Quantum Electron.*, vol. 28, pp. 93–108, 1992.

[4] E. Cerboneschi, F. de Tomasi, and E. Arimondo, "Low-frequency fluctuation instabilities in diode lasers with optical feedback," *Nonlinear Dynamics in Lasers and Optical Systems*, SPIE, vol. 2099, pp. 183–191, 1993.

[5] E.-K. Lee, H.-S. Pang, J.-D. Park, and H. Lee, "Bistability and chaos in an injection-locked semiconductor laser," *Phys. Rev. A*, vol. 47, pp. 736–739, 1993.

[6] T. B. Simpson, J. M. Liu, V. Kovanis, A. Gavrielides, and C. M. Clayton, "Four-wave mixing, nonlinear dynamics and noise in laser diodes," *Chaos in Optics*, SPIE, vol. 2039, pp. 23–34, 1993
[7] L. Goldberg, H. F. Taylor, A. Dandridge, J. F. Weller, and R. O. Miles, "Spectral characteristics of semiconductor lasers with optical feedback," *IEEE J. Quantum Electron.*, vol. QE-18, pp. 555–564, 1982.
[8] R. W. Tkach and A. R. Chraplyvy "Regimes of feedback effects in 1.5-μm distributed feedback lasers," *J. Lightwave Technol.*, vol. LT-4, pp. 1655–1661, 1986.
[9] F. Mogensen, H. Olesen, and G. Jacobsen, "Locking conditions and stability properties for a semiconductor laser with external light injection," *IEEE J. Quantum Electron.*, vol. QE-21, pp. 784–793, 1985.
[10] G. H. M. van Tartwijk, G. Muijres, D. Lenstra, M. P. van Exter, and J. P. Woerdman, "The semiconductor laser beyond the locking range of optical injection," *Electron. Lett.*, vol. 29, pp. 137–8, 1993.
[11] D. Lenstra, G. H. M. van Tartwijk, W. A. van der Graaf, and P. C. De Jagher, "Multi-wave mixing dynamics in a diode laser," *Chaos in Optics*, SPIE, vol. 2039, pp. 11–22, 1993.
[12] G. H. M. van Tartwijk and D. Lenstra, "Nonlocking behavior of an optically injected diode laser," *Nonlinear Dynamics in Lasers and Optical Systems*, SPIE, vol. 2099, pp. 89–99, 1993.
[13] H. Nakajima and R. Fray, "Intracavity nearly degenerate four-wave mixing in a (GaAl)As semiconductor laser," *Appl. Phys. Lett.*, vol. 47, pp. 769–771, 1985.
[14] R. Nietzke, P. Panknin, W. Elsässer, and E. O. Göbel, "Four-wave mixing in GaAs/AlGaAs semiconductor lasers," *IEEE J. Quantum Electron.*, vol. 25, pp. 1399–1406, 1989.
[15] J. G. Provost and R. Frey, "Cavity-enhanced highly nondegenerate four-wave mixing in GaAlAs semiconductor lasers," *Appl. Phys. Lett.*, vol. 55, pp. 519–521, 1989.
[16] S. Murata, A. Tomita, J. Shimizu, M. Kitamura, and A. Suzuki, "Observation of Highly nondegenerate four-wave mixing (>1 THz) in an InGaAsP multiple quantum well laser," *Appl. Phys. Lett.*, vol. 58, pp. 1458–1460, 1991.
[17] P. Schanne, H.-J. Heinrich, W. Elsässer, and E. O. Göbel, "Optical bistability and nearly degenerate four-wave mixing in a GaAlAs laser under intermodal injection," *Appl. Phys. Lett.*, vol. 61, pp. 2135–2137, 1992.
[18] S. Jiang and M. Dagenais, "Nearly degenerate four-wave mixing in Fabry–Perot semiconductor lasers," *Opt. Lett.*, vol. 18, pp. 1337–1339, 1993.
[19] G. P. Agrawal and I. M. I. Habbab, "Effect of four-wave mixing on multichannel amplification in semiconductor laser amplifiers," *IEEE J. Quantum Electron.*, vol. 26, pp. 501–505, 1990.
[20] M. W. McCall, "Enhanced multiwave mixing interactions in semiconductor optical amplifiers via pump modulation," *IEEE J. Quantum Electron.*, vol. 28, pp. 9–15, 1992.
[21] K. Kikuchi, M. Kakui, C.-E. Zah, and T.-P. Lee, "Observation of highly nondegenerate four-wave mixing in 1.5 μm traveling-wave semiconductor optical amplifiers and estimation of nonlinear gain coefficient,"*IEEE J. Quantum Electron.*, vol. 28, pp. 151–156, 1992.
[22] A. D'Ottavi, E. Iannone, A. Mecozzi, S. Scotti, P. Spano, J. Landreau, A. Ougazzaden, and J. C. Bouley, "Investigation of carrier heating and spectral hole burning in semiconductor amplifiers by highly nondegenerate four-wave mixing," *Appl. Phys. Lett.*, vol. 64, pp. 2492–2494, 1994.
[23] R. Lang and K. Kobayashi, "External optical feedback effects on semiconductor injection laser properties," *IEEE J. Quantum Electron.*, vol. QE-16, pp. 347–355, 1980.
[24] J. Dellunde, M. C. Torrent, C. R. Mirasso, E. Hernández-García, and J. M. Sancho, "Analytical calculations of switch-on time and timing jitter in diode lasers subjected to optical feedback and external light injection," *Opt. Commun.*, vol. 115, pp. 523–527, 1995.
[25] L. Li and K. Petermann, "Small-signal analysis of optical-frequency conversion in an injection-locked semiconductor laser," *IEEE J. Quantum Electron.*, vol. 30, pp. 43–48, 1994.
[26] B. Tromborg and J. Mørk, "Nonlinear injection locking dynamics and the onset of coherence collapse in external cavity lasers," *IEEE J. Quantum Electron.*, vol. QE-26, pp. 642–654, 1990.
[27] H. Temkin, N. A. Olsson, J. H. Abeles, R. A. Logan, and M. B. Panish, "Reflection noise in index-guided InGaAsP lasers," *IEEE J. Quantum Electron.*, vol. QE-22, pp. 286–293, 1986.
[28] B. Tromborg, H. Olesen, X. Pan, and S. Saito, "Transmission line description of optical feedback and injection locking for Fabry-Perot and DFB lasers," *IEEE J. Quantum Electron.*, vol. QE-26, pp. 1875–1889, 1987.
[29] F. de Tomasi, E. Cerboneschi, and E. Arimondo, "Asymmetric pulse shape in the LFF instabilities of a semiconductor laser with optical feedback," *IEEE J. Quantum Electron.*, vol. 30, pp. 2277–2280, 1994.
[30] K. Petermann, *Laser Diode Modulation and Noise*. Dordrecht, The Netherlands: Kluwer Academic, 1988.
[31] N. Schunk and K. Petermann, "Noise analysis of injection-locked semiconductor injection lasers," *IEEE J. Quantum Electron.*, vol. QE-22, pp. 642–650, 1986.
[32] M. P. van Exter, W. A. Hamel, J. P. Woerdman, and B. R. P. Zeijlmans, "Spectral signature of relaxation oscillations in semiconductor lasers," *IEEE J. Quantum Electron.*, vol. 28, pp. 1470–1478, 1992.

Elena Cerboneschi, photograph and biography not available at the time of publication.

Daniel Hennequin, photograph and biography not available at the time of publication.

Ennio Arimondo, photograph and biography not available at the time of publication.